IEEE Access
Multidisciplinary | Rapid Review | Open Access Journal

Received March 23, 2020, accepted April 5, 2020, date of publication April 8, 2020, date of current version April 23, 2020.

Digital Object Identifier 10.1109/ACCESS.2020.2986482

The Development of Electrical Tree Discharge in Epoxy Resin Impregnated Paper Insulation

YONGQIANG WANG[1], CHANGHUI FENG[1], AND YU LUO[2]
[1]Hebei Provincial Key Laboratory of Power Transmission Equipment Security, North China Electric Power University, Baoding 071003, China
[2]Shenzhen Power Supply Bureau Company, Ltd., Shenzhen 518000, China

Corresponding author: Yongqiang Wang (qianghd@126.com)

ABSTRACT An electrical tree discharge model of multilayer insulation paper was prepared, and a voltage of 20 kV was used for electrical tree cultivation and initiation tests. Based on the microscopic image information and partial discharge (PD) information during the aging of the electrical tree, the development of electrical tree discharges between layers of paper comprising epoxy resin-impregnated paper insulation was studied. The results show that, by analysing PD information such as the discharge volume phase spectrum and the discharge repetition rate phase spectrum, the development of the electrical tree branch progresses in four stages: initial, growth, stagnation, and bursting. During the growth and stagnation stages, the main discharge paths of the electrical tree are mainly formed, and there are many filamentous fibres on the path edge. During the burst stage, more branches will be formed on the electrical tree, which will cause the greatest damage to the insulation. With the extension of the electrical tree path, the discharge magnitude and discharge times also increase. There are specific discharge patterns in different growth stages of the electrical tree, and the number of discharge events in each positive half-cycle is significantly greater than that in a negative half-cycle. Combining the microscopic image information and PD information during the aging of such an electrical tree, a theoretical basis for evaluating insulation state by PD monitoring is realised. The long-chain molecules of cellulose and epoxy resin break bonds and oxidise, which decompose into a large number of free radicals, monosaccharides, and other low-molecular-weight products.

INDEX TERMS Partial discharge, electrical tree, growth characteristics, epoxy resin-impregnated paper, micromorphology, Fourier transform infrared spectroscopy.

I. INTRODUCTION

With the continuous expansion of societal demand for electrical energy, the voltage of transmission lines has also continued to increase, and the insulation performance of electrical equipment has been severely tested. With the continuous advance of urban construction, dry insulation using epoxy resin casting is gradually being more widely used due to its advantages such as being environmental-friendly and having high electrical strength [1]. As the core electrical equipment in a DC transmission system, the converter transformer's insulation performance on the valve side bushing has withstood significant tests; not only must it withstand the effects of AC electric field, DC electric field, and polarity reversal electric field, but also the severe heating problem caused by the many higher harmonics in the system. Under the long-term action of high temperature and high pressure, the valve bushing of the converter transformer is prone to insulation degradation, affecting the safe, stable operation of the converter transformer. Epoxy resin-impregnated paper insulation is prone to aging discharge breakdown of its electrical tree under multi-factor long-term effects imposed by such a complex environment, which causes the solid insulation performance of the equipment to be severely reduced, never to be recovered [2], [3].

Electrical trees are small, tree-like paths formed by cracks in the internal discharge of electrical equipment during operation. The paths are empty and there are carbon particles on the wall of the discharge region. The charged particles generated by the PD collide with the insulating material. In time, the molecular chains are cut off, rapidly oxidised, and decomposed into small molecules or gases inside the insulating material, forming fine corrosion paths, namely an electrical tree. When electrical tree branches develop, they

The associate editor coordinating the review of this manuscript and approving it for publication was Boxue Du.

cause a breakdown in equipment insulation, resulting in large-scale power failure. As for those factors that affect the electrical tree discharge of insulating materials, currently, they include the molecular structure of the material, changes in the temperature and humidity of the environment, the curing reaction process, the casting process, the interaction between different materials, and the electrode materials in the experiment [4], [5]. Once electrical tree discharges occur in a solid insulation material, the insulation performance of the casing will be irrecoverable, seriously threatening the safety of the converter.

Since electrical tree is one of the main factors for ageing of electrical insulation, scientists have carried out research on the development of electrical tree of various electrical insulating materials. B. Du has done a lot of research on the development of electric tree of epoxy resin under various test environments [6]–[8]. T. Han *et al.* focused on electrical tree in silicone rubber with temperature gradient under repetitive pulse voltage [9]. Y. Zhou *et al.* studied electrical tree initiation of silicone rubber after thermal aging [4]. Y. Liu *et al.* studied electrical tree initiation in cross-linked polyethylene under constant DC, grounded DC, and at elevated temperature [10]. M. Liu *et al.* focused on growth and partial discharge characteristics of electrical tree in cross-linked polyethylene under AC-DC composite voltage [11]. Alternatively, in order to characterize the overall structure of electrical tree patterns during their growth, scientists have been using have used many methods. Image analyses by pixel counting to characterize tree growth have also been carried out by Yoshimura *et al.* [12]. Partial discharge behavior, has been shown to reflect tree growth characteristics, with new growth occurring at those parts of the tree in which the partial discharges are visible [13]. The study of the development of electrical tree discharge in dielectrics can depends on image observation methods [14].

Although there have been many analytical studies of the phenomenon of electrical tree structure in insulating materials, but there are few studies on electrical trees using epoxy resin-impregnated insulating paper insulation, especially on the development of electrical trees between paper layers. Therefore, in the present work we used the traditional pin-plate electrode model to study electrical tree characteristics between dry-insulated multilayer papers at room temperature. The morphological structure, growth characteristics, partial discharges, and micro-morphology of the electrical tree branch discharge path were analysed to reveal the development of electrical tree discharges between multiple layers of insulation paper.

II. SAMPLE PREPARATION EXPERIMENTAL AND TEST METHOD

A. SAMPLE PREPARATION

In this experiment, a square electrical tree discharge sample with a side length of 25 mm was made. The needle electrode was placed between two layers of insulating paper in advance to simulate the electrical tree discharge defect between paper and paper. In this experiment, a high-activity, low-viscosity liquid bisphenol A diglycidyl ether (E-51 type) produced by Shanghai Resin Factory was used. The curing agent was a modified aliphatic amine. The curing agent was a mixture containing primary amine and secondary amine, and the accelerator was DMP-30. The mixed epoxy resin solution is colourless and transparent, which is convenient when observing the development of, and changes in, the shape of the electrical tree.

The insulation paper was first cut into squares with a side length of 25 mm, and these were dried in a vacuum drying box at 110 °C under a pressure of 50 Pa for 48 h to remove the moisture present in the insulation paper and test the moisture content of the insulation paper by Karl Fischer titration to ensure that the initial moisture content of the insulating paper is less than 0.5 %, thus reducing the error in each sample. If too many sheets of insulating paper are used in the sample model, the colour will be deepened, which will impair observation of the development of electrical tree morphology. Therefore, here we used a two-layer insulating paper model, and the needle electrode was placed in the middle of the insulating paper in advance. Among them, the customised stainless-steel needle electrode had a diameter of 0.3 mm, the angle of the needle tip was about 30°, and the radius of curvature of the needle tip was about 2 μm. The distance between the sample needle tip and the bottom of the sample model was 6 mm, to ensure that there were no bubbles or stress concentration near the embedded needle point. The outside of the two layers of insulating paper was sealed by a colourless, highly-transparent acrylic plate with a thickness of 3 mm. The ground electrode was made of copper foil connected to the ground wire, and the epoxy resin sample and the copper plate electrode were fixed by EVA glue. A diagram of the electrical tree sample model is shown in Fig. 2, and the system measured 25 mm × 25 mm × 6 mm.

The entire sample model was cast with an epoxy resin solution. The epoxy resin solution was prepared according to a mass ratio of epoxy resin and curing agent of 4:1. The epoxy resin and curing agent were weighed on a high-precision electronic scale, and then mixed in a clean beaker. The mixture was evenly and rapidly stirred for 10 min by magnetic agitator. A mould (Fig. 1) is then used to cast the electrical tree sample, where the needle electrode is placed in the mould before pouring. Then we placed the insulating paper and the acrylic board of the same size in the mould in that order, and then cast the epoxy resin mixed solution. The whole was placed in a vacuum drying box, maintained at a temperature of 25 °C, and evacuated for 1 h to remove water vapour and air from the epoxy resin solution. Then the specimen was placed in a dry box for 3 h at room temperature and the mould removed.

B. PD EXPERIMENT PLATFORM

As shown in Fig. 3, the PD platform is composed of a power frequency high voltage test control system, a PD

FIGURE 1. The cast epoxy resin mould.

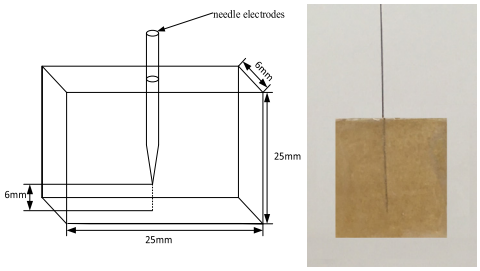

(a) Structural drawing of the sample model (b) Drawing of the sample

FIGURE 2. Drawing of the sample model.

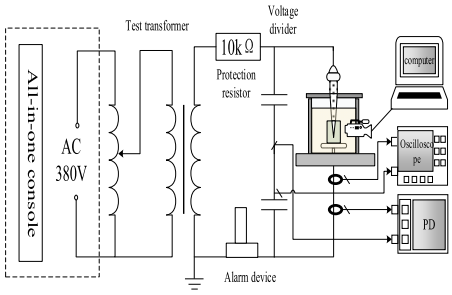

FIGURE 3. Schematic diagram of the PD test platform.

detection system and an image real-time observation system [15]. The power frequency high voltage test control system adopts YDTW-10/100 oil-immersed non-halo test transformer, which is at the rated operating voltage. The apparent discharge of PD is less than 5 pC and the rated power is 10 kVA. The resistance of the protection resistor is 10 kΩ, and the capacitance of the capacitive voltage divider is 1000 pF, which plays a role of current limiting protection when the sample is broken down, thereby protecting the testing equipment from being damaged during the moment of the test breakdown. The divider ratio of the capacitor divider is 1000 : 1, which is used to collect reference voltage signals. The PD detection system used the HCPD-2622 digital partial discharge patrol instrument to detect the PD signal by a pulse current method with a sampling frequency of 20 MHz. During the partial discharge test, the signals detected by the partial discharge detection system are connected to the partial discharge inspection instrument to collect and record the discharge signals. The real-time image observation system includes an optical microscope and a charge-coupled component camera system (CCD camera system), which are used to capture the image of the electrical tree, and analyze the start, development process and tree shape of the electrical tree. The microscope is connected to a computer through a corresponding CCD camera system, which can observe the initiation and growth of electrical tree in real time. The microscope system used in this paper uses a high-magnification continuous-magnification single-tube video microscope. The continuous magnification range of the microscope's main body is from 1 to 6.5. In this experiment, the magnification of eyepiece is 10, the magnification of main body is 5, and the magnification of the objective lens is 0.75. The visual magnification is 37.5, and with the CCD camera system, the video magnification is 222.5. Before the test, the microscope system was calibrated using a microscope scale with a minimum graduation of 10 μm. The experiment was about 388 pixels per 1 000 μm.

The ambient temperature of the experiment is 25 °C, the testing accuracy of the PD meter reached ± 1 pC, and the central bandwidth can be independently selected, which meets the detection requirements of PD in the electrical tree experiment. The PD detection device is placed in a shielded room and calibrated before the experiment, to pre-process the interference factors present in the environment within which the experiment is located. Without placing the sample, the PD in the environment is within 5 pC during the step-up from 0 kV to 20 kV. In this experimental range, the measuring device meets the requirements of IEC 60207, which ensures that the signal detected in the experiment originates from the sample's own discharge.

In this test, a strong light source was used to irradiate from the opposite side of the sample to ensure that the development of an electrical tree between insulating paper and insulating paper could be clearly observed. After the PD detection device is calibrated, the sample is positioned and the real-time image observation system is opened. At room temperature, a culture test was performed on the electrical tree discharges insulated between insulating papers, with five samples per group. The specific process is as described below.

The experiment uses a constant voltage method to slowly increase the voltage at a rate of 0.1 kV/min. After the discharge signal appears, the voltage remains unchanged for 10 min. If there is still a stable discharge signal at that time, this voltage is the initial discharge voltage U of the sample. If the applied voltage is too high, the discharge process appears violent, and the growth of the electrical tree is too fast. It is too late to record and is prone to breakdown, causing the electrical tree path to be completely carbonised. If the applied voltage is too low, the discharge is not obvious, and the pressing time is long, which is also not conducive to the growth of the electrical tree. After several experiments, the test voltage of 20 kV is more reasonable for the cultivation of an electrical tree. After the voltage is increased to 20 kV, the voltage is maintained, and electrical tree cultivation is performed at that voltage. An electrical tree exceeding 10 μm

in length was used as the criterion for judging the electrical tree growth; however, due to the rapid growth of the electrical tree, the length of the electrical tree was greater than 10 μm when the PD was greater than 15 pC for the first time. Therefore, in this experiment, the discharge exceeding 15 pC for the first time was used as the criterion for judging electrical tree growth.

III. RESULTS AND ANALYSIS

A. THE DEVELOPMENT OF ELECTRICAL TREE BRANCHES BETWEEN MULTIPLE LAYER OF INSULATION PAPER

Here, a PD detection system and a real-time image observation system are used to study the development process of an electrical tree between multilayer insulating paper. According to the growth morphology of the electrical tree, the discharge volume phase spectrum and the discharge repetition rate phase spectrum, the development process of the electrical tree is divided into initial, growth, stagnation, and burst stages. At present, the study of electrical trees in dielectrics mainly depends on image observation methods [14]. Combined with such images, researchers were able to ascertain many of the growth characteristics and patterns associated with an electrical tree. Fig. 4 shows the growth morphology of electric branches between multilayer insulating paper at different stages of development. Table 1 lists the duration of different stages of electrical tree discharges.

TABLE 1. Division of electrical tree discharge stages.

Stage	Initial	Growth	Stagnation	Burst
Division/ min	0 to 60	60 to 300	300 to 400	400 to breakdown

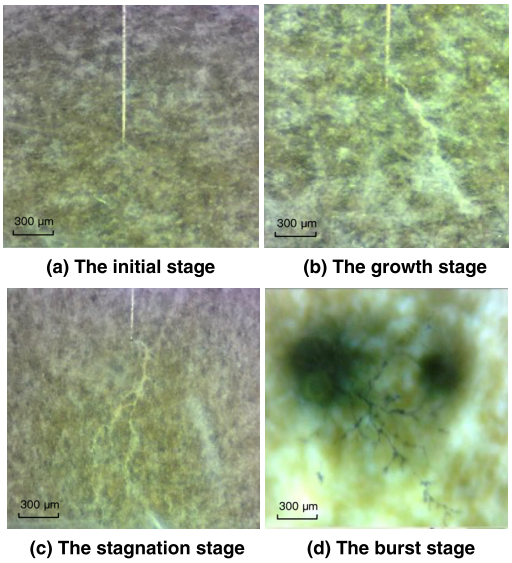

FIGURE 4. Morphology of a developing electrical tree.

Fig. 4(a) shows the initial stage of the electrical tree discharge. The PD signal was very weak in the initial stage, and no obvious continuous discharge signal could be detected [11]. After about 60 min of voltage application, a relatively stable discharge signal will appear. When the length of the first electrical tree path reaches 10 μm, this process is called the initial stage of electrical tree development. Although no obvious electrical tree path can be observed at this stage, a PD signal has been generated, evincing a non-destructive PD process.

Fig. 4(b) shows the growth stage of the electrical tree discharges. After about 300 min of voltage application, a clear discharge path can be seen under the microscope. During the growth stage, the main discharge path of the electrical tree develops along the needle tip towards the ground electrode. The main discharge path has few bifurcations, and the main shape is that of a single branch. This is because the continuous partial discharge of the needle tip, high-energy electrons hit the insulating molecules at the front end of the needle tip under the action of an electric field, causing the molecular chain to break and cause local degradation, generating free radicals, accompanied by oxidation reactions. Micro-paths then appeared, forming light-coloured branches.

Fig. 4(c) shows the stagnation stage of the electrical tree discharges. When the pressure had been applied for about 400 min, the discharge will be relatively stable. Under the microscope, it can be observed that some small branch discharge paths will appear in the main discharge path, and the branch paths will become denser in the burst stage. The shape of the electrical tree gradually changes from that of a single branch to multiple branches, but the development of the electrical tree path is slow, and the main discharge path is no longer extended. This is because during the development of the primary path of the electrical tree, many space charges will be formed around it. The presence of space charges will weaken the applied electric field, which will decrease the rate of charge extraction and injection. The destructive effect of the electric field itself weakens, which causes the development of the electrical tree to slow down. The energy released by the discharge is not sufficient to maintain the continuous breakdown of the tip of the tree, resulting in the stagnation of the main discharge path of the electrical tree.

Fig. 4(d) shows the burst stage of the electrical tree discharges. When the pressure has been applied for about 480 min, the degree of discharges increases continuously and becomes very dense. The branches produced by the discharge also become very dense and develop in all directions. The main discharge path continues to develop. The path of the electrical tree has also undergone carbonisation, making its ''branch'' thicker, the colour deeper, and its continuous development to the ground electrode eventually leads to insulation breakdown. This is because the PD formed by the long-term injection and extraction of free electrons will cause the temperature at the discharge point to rise, the free electrons to accelerate, and the kinetic energy to increase. Under the action of the high temperature and high field strength, high-energy electrons collide with gas molecules to produce more free electrons, forming an electron avalanche, and

electrical tree develops rapidly. At the same time, the diffusion behaviour of space charges will lead to bifurcation of the electrical tree. With the gradual increase and accumulation of bifurcations, cluster-like electrical trees appear at the front end of the needle tip, and the front end of each clustered electrical tree will continue to branch, tending to generate cluster s of branches.

B. ANALYSIS OF PD PHASE SPECTRUM

At present, the aging characteristics of electrical tree in insulating materials are mainly studied through image observation methods. The laws and characteristics of electrical tree growth can be obtained through image observation methods such as microscopes and SEM. At the same time, because the relevant information of PD is closely related to the insulation condition of electrical equipment, the potential operation defects and insulation deterioration of electrical equipment can be found according to the relevant information of PD measurement [16]. Authorities in the international electrical field, such as IEC, IEEE and CIGRE, all recommend PD tests as the best method for evaluating insulation status. The related research on the aging of electrical tree of insulating materials shows that there is a very obvious phenomenon of PD during the growth of electrical tree. According to the spectrum information of PD, the discharge degree of electrical tree of solid insulating materials can be evaluated reasonably [17].

The discharge phase and amplitude sequence of the PD signal at different stages of the electrical tree discharges are plotted in a two-dimensional coordinate system in the form of dot, and a two-dimensional discharge volume-discharge phase (q-φ) scatter diagram [18], [19] is obtained (Fig. 5). The scatter points in the PD spectrum represent the PD signal, and the different colours on the scatter points represent the change in the number of PD events (where yellow indicates a high number of PD events). The vertical coordinate of the spectrum shows the discharge intensity, and the amplitude indicates the intensity of discharges. Although the distribution of each point in the scatter diagram appears chaotic and cannot be represented by a simple functional relationship, the data in the diagram have not been post-processed, so as to reflect the dispersion of the discharge, and implies the similarity between the discharge amplitude and discharge phase. Therefore, the q-φ scatter diagram shows both the concentrated and scattered parts of the discharge pulse in the q-φ plane. It can not only reflect a single PD event, but also show its statistical regularity to a large extent.

During the initial stage of the electrical tree discharges, the discharge is mainly concentrated at about 25 pC. The PD signal detected at this stage suggests a small discharge per voltage cycle (Fig. 5(a)). In this stage, because of the dense arrangement of fibres, high degree of order, and good electrical performance of the insulation, the discharge remained small. In the initial stage, high-energy electrons continuously bombarded epoxy and fibre molecules, destroying their insulating properties. During the growth stage, the discharge increases to a relatively stable state at around 850 pC

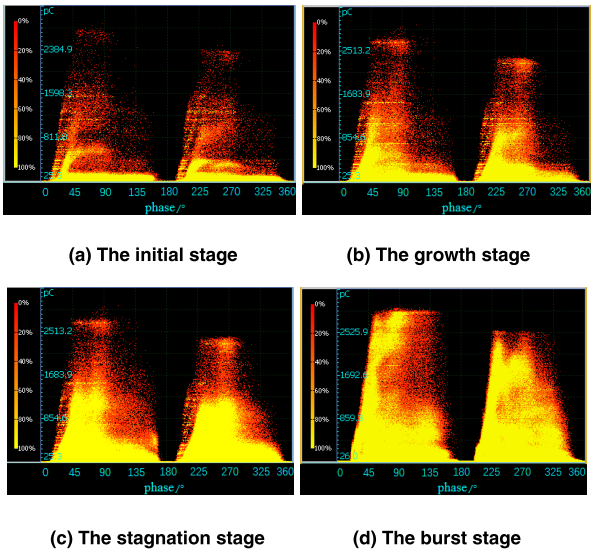

(a) The initial stage (b) The growth stage

(c) The stagnation stage (d) The burst stage

FIGURE 5. The q-φ scatter diagram at different stages of PD development.

(Fig. 5(b)). This stage represents the development of the primary path of the electrical tree discharges, and it is also the main stage in which the destruction of the insulating material by the electrical tree discharge occurs. During the stagnation stage, the discharge is mainly concentrated around 1680 pC, and the discharge phase distribution is triangular (Fig. 5(c)). In this stage, a low-amplitude discharge will appear intermittently. Since the channel is uniformly distributed around the initial channel, the electric field intensity is more uniformly influenced by the shielding effect of branching and the surrounding space charge [20]. The growth of the electrical tree towards the low-voltage electrode is limited to a certain extent, resulting in the emergence of a stagnation stage. Although the channel of the electric tree did not continue to develop in a forward direction, the discharge process continued, so from the growth stage to the stagnation stage, the discharge still increased. During the burst stage, a large discharge occurs at about 2800 pC, and the discharge phase is spread throughout the interval (Fig. 5(d)). Many high-energy electrons in the branch path collide and ionise under the action of the high-strength electric field, producing more free electrons and forming an electron avalanche. When the high-speed electrons reach the top of the tree branch, and their quantity and speed reach a certain level, numerous severe collisions and dissociation will cause many polymer molecular bonds to be broken, resulting in severe burning of the path wall, a high degree of carbonisation, and severe discharges.

Fig. 6 shows the change in discharge amount during PD. Throughout the discharge process, the discharge data collected by the PD patrol instrument were counted to obtain the variation in mean average discharges (q_{ave}) at 30-min intervals. It can be seen from the figure that the average value of PD increases only slightly within 0 min to 120 min of voltage application. The discharge amount will increase from

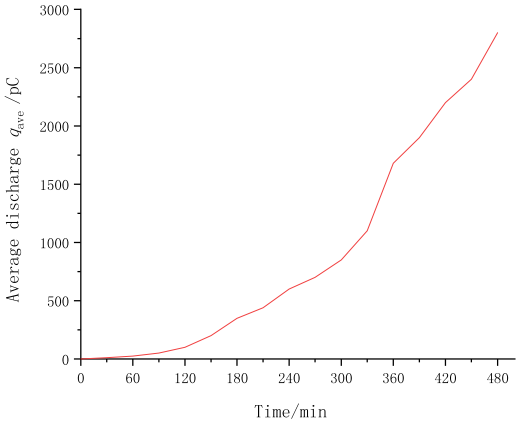

FIGURE 6. The trend in amount of discharge during PD.

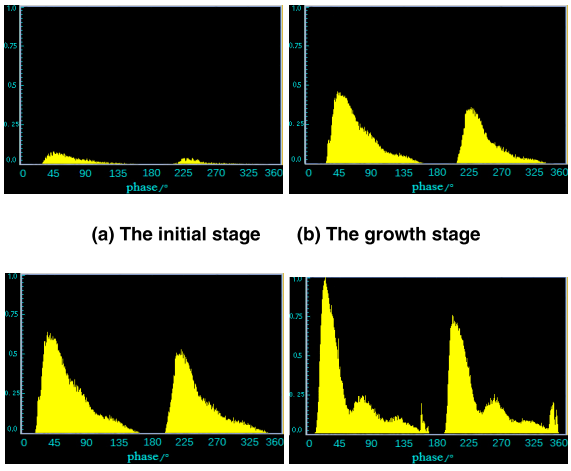

(a) The initial stage (b) The growth stage

(c) The stagnation stage (d) The burst stage

FIGURE 7. The discharge repetition rate phase spectrum at different stages of PD development.

120 min to 330 min and thereafter, the amount of discharge amount will increase rapidly.

C. ANALYSIS OF THE DISCHARGE REPETITION RATE PHASE SPECYRUM

In the PD spectrum, the discharge repetition frequency n represents the number of PD events per unit time, usually expressed as the average number of pulses of PD per second. A power frequency cycle is divided into several phase windows, and the discharge repetition frequency n is regarded as a function of phase φ. The n-φ histogram can be plotted to reflect the distribution of discharge repetition frequency with phase. Fig. 7 shows the discharge repetition rate phase spectrum of the electrical tree between multiple layers of insulating paper. The amplitude of n is normalised according to the following formula [21]:

$$\eta = \frac{\lambda}{\lambda_{\max}}, \quad \eta \in [0, 1]$$

where η is the normalized value, λ refers to the value before the normalization process, and $\lambda_{\max}$ is the maximum value in the experimental data.

The discharge repetition rate phase spectra corresponding to the four stages of electrical tree development are all ''peak shaped'', and the number of discharges in the positive half-cycle is significantly larger than that in the negative half-cycle. During the initial stage of electrical tree discharges, the discharge is mainly concentrated in the phase intervals from 30° to 90° and 220° to 240°. The amount of discharges is relatively weak, and the number of corresponding discharge events is reduced (Fig. 7(a)). During the growth stage, the concentration of discharges is extended to between 30° to 140° and 220° to 320°. Compared with the initial stage, the amount of discharges and the number of discharge events in this stage are significantly increased, and the degree of discharges is severe, causing the most insulation damage (Fig. 7(b)). During the stagnation stage, compared with the growth stage, the discharge does not fluctuate to any significant extent, the discharge phase interval remains unchanged, and intermittent PD events occur (Fig. 7(c)). During the burst stage, with the continuous development of the main discharge path and branches, the severity of collision ionisation and discharge continues to increase, and a large discharge signal will appear in a specific phase interval (Fig. 7(d)).

According to the aforementioned analysis, the discharge amount and the number of discharge events increase with the extension of the electrical tree path. The electrical tree exhibits specific discharge patterns in different growth stages. Based on the maximum test data in the experiment, the amplitude of the discharge repetition frequency is uniformly normalized according to the formula. The discharge amount with a smaller amplitude becomes very small after the normalization process, and the undischarged phase may be shown in Fig. 7. Therefore, there is much difference in the non-discharge interval in the four stages in Fig. 7. The number of discharge events in the positive half-cycle is significantly greater than in the negative half-cycle. This is because, in the positive half-cycle, the development of the discharge process will lead to the generation of many space charges: in the negative half-cycle, the presence of the space charges will inhibit development of the discharge process, thus slowing the rate of charge extraction and injection speed, and reducing the degree of discharges. During the growth stage of electrical tree discharges, the discharge is determined by the applied electric field, however, during the lag stage of the electrical tree branch, the space charge previously formed in the path weakens the applied electric field. At this time, the discharge is determined by the composite electric field superimposed both inside and out, therefore, electrical tree discharges will enter a short stage of stagnation, and the rate of development of the electrical tree discharge path will decrease, as will the discharge speed. This is because there will be intermittent low-amplitude discharges in the electrical tree branches during the stagnation stage, which provide the initial electrons needed to form strong discharges during the burst stage.

At the same time, the electric field strength at the front end of the electrical tree will increase rapidly due to the decrease in the distance from the ground electrode, which will cause the growth of the electrical tree. The free electrons remaining in the discharge path are re-initiated and sustained by the high-strength electric field. When the electron concentration at the tip of the needle is sufficiently large, more fine branches will develop at the tip of the needle to form new cluster branches and this is thus reflected in the discharge events being n more numerous and more intense. According to the distribution of PD signals, the development stage of electrical tree path and the density of the electrical tree can be reflected to some extent.

D. ANALYSIS OF THE MICRO-MORPHOLOGY OF THE LONGITUDINAL SECTION OF THE ELECTRICAL TREE PATH

To explore the development of electrical trees in the multilayer paper insulated by epoxy resin-impregnated paper, the scanning electron microscope (SEM) of EM-30 plus was used (at 50× magnification) to observe the micro-morphology of the longitudinal section of the electrical tree path between multiple layers of papers. The branch shape, tip front end, and breakdown path morphology of electrical tree discharges are measured respectively (Fig. 8).

During the initial stage of the growth of the electrical tree, the discharge path of the electrical tree develops along the path between the insulating paper layers. Electrical trees are less likely to break through the insulating paper surface and develop to the other side. It can be seen (Fig. 8(a)) that during the growth stage, because the degree of discharges is not as severe as that in the burst stage, many filamentous fibres are visible at the edge of the discharge path of the electrical tree. The originally dense fibres were continuously bombarded with high-energy electrons under the action of the extremely uneven electric field at the tip of the needle, and electrical dendritic discharge paths appeared. Fig. 8(b) shows the discharge path at the tip: the average width of the discharge path at the tip of the tip is about 1300 um. Fig. 8(b) shows the discharge path at the tip: the average width of the discharge path is measured to be about 1300 um. It can be seen that the fibres at the tip of the needle are more scattered and fluffier than those filamentous fibres seen at the edge of the discharge path of the electrical tree. At the same time, each of the filamentous fibres maintains a certain separation, and do not overlap. This is because each filamentary fibre contains many space charges with the same sign, which causes each filamentary fibre to repel another. Figs 8(c) and (d) show SEM micrographs of the primary path after the breakdown of the electrical tree. When the tiny electrical tree path approaches the ground electrode, the PD will continue to erode the insulating material, making the electrical tree path wider and leading the high-voltage end to the treetops. The needle electrode, that is, the high-voltage electrode, will be grounded instantly. A large current flow through the electrical tree path causes insulation breakdown. At this time, the average width of the primary path for the breakdown of the electrical tree was about 1950 um, which is about 600 μm wider than that of the discharge path at the front of the tip. The electrical tree path is wide and has the highest degree of carbonisation, which will form a visible discharge path and destroy the insulating material [22]. The intense discharge will burn out the filamentous fibres at the edge of each fibre, making the edge of the discharge path

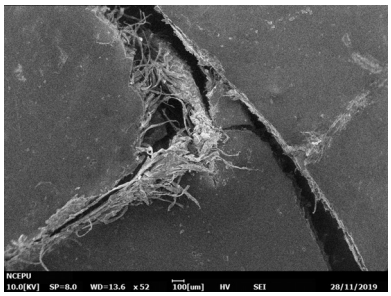

(a) The branch shape path

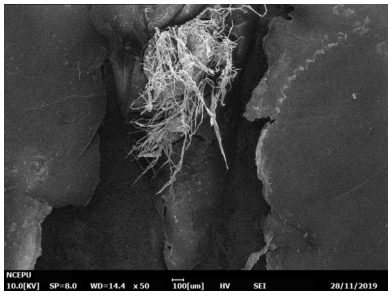

(b) The tip front path

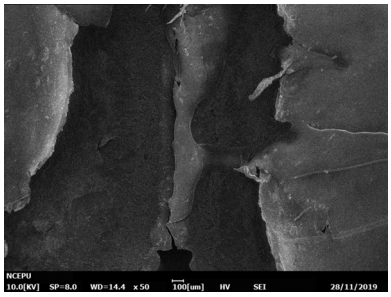

(c) Breakdown path 1

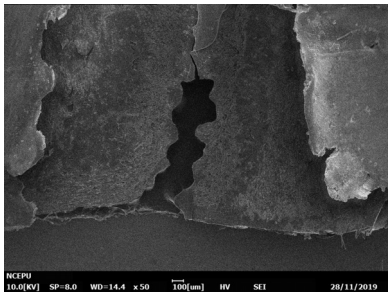

(d) Breakdown path 2

FIGURE 8. The micro-morphology of the longitudinal section of the electrical tree path.

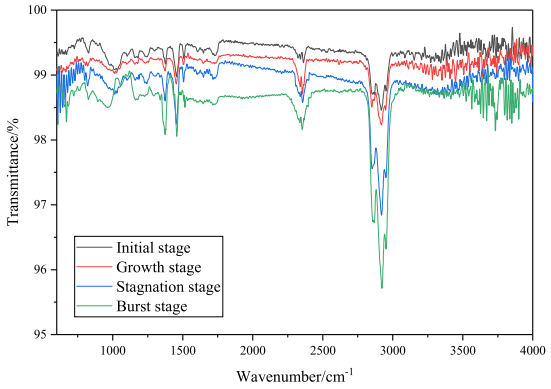

FIGURE 9. FTIR spectra of samples in different stages of electrical tree development.

smoother. After the breakdown of the discharge, the discharge path of the electrical tree will even develop horizontally, and then develop to another layer of insulating paper through the breakdown path afforded by the insulating paper. There will be visible gullies formed under the main discharge path (Fig. 8(d)). The width of the discharge path is about 350 μm therein and because the dry insulation is impregnated with epoxy resin, the bonding between fibres is tighter, breaking of, or detachment from, the fibre body is seen. Therefore, the surface of the discharge path remains relatively smooth.

E. ANALYSIS OF INFRARED FOURIER SPECTRA

Infrared examination of insulation samples was performed using a Nicolet iS5 model Fourier infrared spectrometer (Thermo Fisher Scientific). The test conditions are as follows: room temperature 20 °C at a relative humidity of less than 50 %. The number of scans in this FTIR test is set to 32, the resolution is 4.0 cm^{-1}, and the wave number ranges from 600 to 4 000 cm^{-1}. The final scan results are shown in transmittance terms, and a background air scan was conducted before each sample measurement to eliminate external interference. To compare the change in the infrared peak more clearly, the infrared image of the sample at different development stages were selected for analysis in this section (Fig. 9).

In the range of wave numbers from 1650 to 1700 cm^{-1}, with the development of an electrical tree, the transmittance of the insulation sample decreases. This indicates that, with the development of the electrical tree, carbonyl group is produced in the sample. The carbonyl group contains a ketone group, ester group, aldehyde group, carboxyl group, and other functional groups [23]. During development of the electrical tree, the temperature inside the sample increases. Under the synergistic action of external electric field and temperature field, weak bonds (such as those hydroxyl and aldehyde groups on the macromolecular chain in the epoxy resin polymer) break, and free radicals (such as carbonyl groups) are produced [24]. At the same time, under the combined effect of the electric field and temperature field, the alcohol hydroxyl group (-CH_2OH) in the cellulose molecular chain is oxidised to form aldehyde and ketone groups. The carriers produced by PD during the development of the electrical tree will bombard the fibre surface continuously, producing strong-electronegativity intermediates. This can cause the cellulose molecules to continue to be oxidised to form ester or carboxyl groups [25]. In the range of wave numbers from 2800 to 2950 cm^{-1}, a Fermi double-peak appeared; because this band is an aldehyde C-H bond stretching vibration, the presence of aldehyde groups in the molecule can be identified.

The presence of a hydroxyl group, ether group, and active epoxy group in the molecular structure of epoxy resin results in strong intermolecular force between epoxy molecule and the adjacent interface. The epoxy group reacts with the free bond on the surface of the medium to form a chemical bond [26]. With the development of an electrical tree, the main chain of the epoxy resin breaks, and the number of molecular chain breaks increases. Many free radicals are produced by degradation of the samples. Cellulose is formed by aldehyde groups and alcohol hydroxyl groups in the glucose molecules to form C1-C5 glycosidic bonds, which can then form two typical six-ring structures, α-D-glucopyranose and β-D-glucopyranose. Due to the difference in spatial arrangement of these linear compounds, crystalline and amorphous regions are formed. Among them, the number of hydrogen bonds in the crystal region is much greater than that in the amorphous region. The partial discharge occurring in the development of an electrical tree will destroy the glycoside bond and hydrogen bond in cellulose. The structure of the polymer chain will change in the process of cracking and cross-linking [27]. A large number of high-energy electrons in the branch channel undergo collision ionisation under the action of a high-intensity electric field, generating more free electrons, causing many polymer molecular bonds to be broken and decomposed to form a large number of low-molecular-weight products such as free radicals, monosaccharides, and carboxylic acids.

IV. CONCLUSION

(1) The development of electrical tree discharges in multilayer paper insulated with epoxy resin-impregnated paper has undergone initial, growth, stagnation, and burst stages.

(2) The development characteristics of an electrical tree between multiple layers of paper were observed through a microscope. During the growth stage, the primary path discharge is formed. Then the development of the electrical tree has entered a stage of stagnation. In this stage, the inhibition of space charge will decrease the rate of forward extension of the primary path of the electrical tree and cause the development of a few small branches. When the development of the electrical tree enters its burst stage, many clustered electrical trees formed by branch paths in the front of the needle tip are seen. At this time, the development of the electrical tree is rapid, and the path colour is deepened and becomes darker.

(3) PD information pertaining to the discharge phase spectrum and discharge repetition phase spectrum was analysed. During the initial stage, the amount of discharges is relatively weak, and the number of discharge events is small. During the growth stage, the discharge will increase significantly and enter a relatively stable stage and the electrical tree will grow faster. During the stagnation stage, the discharge will appear as intermittent low-amplitude discharges. During the burst stage, the amount of discharge number of discharge events increased further, and the intensity of discharge increased. The number of discharge events in a positive half-cycle was significantly higher than that in a negative half-cycle.

(4) The longitudinal section of the discharge path of the electrical tree was observed using an SEM. Many filamentous fibres appear on the edges of the electrical tree discharge paths formed during the growth stage, and the discharge paths thereon are narrow. Many fluffy filamentous fibres will be formed at the tip of the needle. After the electrical tree path is penetrated, the path becomes wider, and the path and its edges become smoother. The damage to the insulation is obvious.

(5) During the development of an electrical tree, the long-chain molecules of cellulose and epoxy resin break bonds and oxidise, which decompose into many free radicals, monosaccharides, and other low-molecular-weight products.

REFERENCES

[1] Y. Wang, Y. Luo, J. Guan, and R. Ding, "Dielectric properties of epoxy resin impregnated paper insulation in different stages of partial discharge development," *Polym. Composites*, vol. 41, no. 1, pp. 360–368, Jan. 2020.

[2] S. M. Rowland, R. Schurch, M. Pattouras, and Q. Li, "Application of FEA to image-based models of electrical trees with uniform conductivity," *IEEE Trans. Dielectr. Electr. Insul.*, vol. 22, no. 3, pp. 1537–1546, Jun. 2015.

[3] Y. Wang, Y. Luo, and C. Feng, "The influence of temperature and aging on the characteristic parameters of dielectric spectroscopy of epoxy resin impregnated paper insulation," *Macromol. Res.*, vol. 27, no. 10, pp. 1030–1037, Oct. 2019.

[4] Y. Zhou, Y. Zhang, L. Zhang, D. Guo, X. Zhang, and M. Wang, "Electrical tree initiation of silicone rubber after thermal aging," *IEEE Trans. Dielectr. Electr. Insul.*, vol. 23, no. 2, pp. 748–756, Apr. 2016.

[5] B. X. Du and L. W. Zhu, "Electrical tree characteristics of XLPE under repetitive pulse voltage in low temperature," *IEEE Trans. Dielectr. Electr. Insul.*, vol. 22, no. 4, pp. 1801–1808, Aug. 2015.

[6] B. X. Du, L. W. Zhu, and T. Han, "Effect of low temperature on electrical treeing of polypropylene with repetitive pulse voltage," *IEEE Trans. Dielectr. Electr. Insul.*, vol. 23, no. 4, pp. 1915–1923, Aug. 2016.

[7] B. Du, M. Tian, J. Su, and T. Han, "Electrical tree growth characteristics in epoxy resin with harmonic superimposed DC voltage," *IEEE Access*, vol. 7, pp. 47273–47281, 2019.

[8] B. Du, M. Tian, J. Su, T. Han, W. Zhu, X. Kong, and J. Jiang, "DC-impulse voltage-dependent electrical tree growth characteristics of epoxy resin in LN2," *IEEE Trans. Appl. Supercond.*, vol. 29, no. 2, pp. 1–5, Mar. 2019.

[9] T. Han, B. Du, T. Ma, F. Wang, Y. Gao, Z. Lei, and C. Li, "Electrical tree in HTV silicone rubber with temperature gradient under repetitive pulse voltage," *IEEE Access*, vol. 7, pp. 41250–41260, 2019.

[10] Y. Liu, X. Cao, and G. Chen, "Electrical tree initiation in XLPE cable insulation under constant DC, grounded DC, and at elevated temperature," *IEEE Trans. Dielectr. Electr. Insul.*, vol. 25, no. 6, pp. 2287–2295, Dec. 2018.

[11] M. Liu, Y. Liu, Y. Li, P. Zheng, and H. Rui, "Growth and partial discharge characteristics of electrical tree in XLPE under AC-DC composite voltage," *IEEE Trans. Dielectr. Electr. Insul.*, vol. 24, no. 4, pp. 2282–2290, Sep. 2017.

[12] N. Yoshimura, M. Yanagiwara, and L. Guang Fan, "Diagnostics of treeing degradation by image processing," *IEEE Trans. Electr. Insul.*, vol. 26, no. 2, pp. 314–317, Apr. 1991.

[13] J. V. Champion, S. J. Dodd, and J. M. Alison, "The correlation between the partial discharge behaviour and the spatial and temporal development of electrical trees grown in an epoxy resin," *J. Phys. D, Appl. Phys.*, vol. 29, no. 10, pp. 2689–2695, Oct. 1996.

[14] N. Shimizu and C. Laurent, "Electrical tree initiation," *IEEE Trans. Dielectr. Electr. Insul.*, vol. 5, no. 5, pp. 651–659, Oct. 1998.

[15] Y. Zhang, Y. Zhou, L. Zhang, Z. Lin, J. Liu, and Z. Zhou, "Electrical treeing behaviors in silicone rubber under an impulse voltage considering high temperature," *Plasma Sci. Technol.*, vol. 20, no. 5, May 2018, Art. no. 054012.

[16] J. C. Pandey and N. Gupta, "Estimation of interphase thickness of epoxy-based nanocomposites," *IEEE Trans. Dielectr. Electr. Insul.*, vol. 23, no. 5, pp. 2747–2756, Oct. 2016.

[17] R. Schurch, S. M. Rowland, and R. S. Bradley, "Partial discharge energy and electrical tree volume degraded in epoxy resin," in *Proc. IEEE Conf. Electr. Insul. Dielectr. Phenomena*, Oct. 2015, pp. 820–823.

[18] I. Iddrissu, S. M. Rowland, H. Zheng, Z. Lv, and R. Schurch, "Electrical tree growth and partial discharge in epoxy resin under combined AC and DC voltage waveforms," *IEEE Trans. Dielectr. Electr. Insul.*, vol. 25, no. 6, pp. 2183–2190, Dec. 2018.

[19] W. Chang, C. Li, Q. Su, and Z. Ge, "Study on development of partial discharges at the defect caused by a needle damage to a cable joint," *Proc. CSEE*, vol. 33, no. 7, pp. 192–201, 2013.

[20] T. Tanaka, "Space charge injected via interfaces and tree initiation in polymers," *IEEE Trans. Dielectr. Electr. Insul.*, vol. 8, no. 5, pp. 733–743, Oct. 2001.

[21] W. Yongqiang, L. Han, F. Changhui, G. Jie, and G. Yicheng, "Electric tree characteristics of glass fiber reinforced epoxy insulation composites with different contents," *Fibers Polym.*, vol. 20, no. 10, pp. 2207–2214, Oct. 2019.

[22] X. Chen, D. Murdany, D. Liu, M. Andersson, S. M. Gubanski, U. W. Gedde, and Suwarno, "AC and DC pre-stressed electrical trees in LDPE and its aluminum oxide nanocomposites," *IEEE Trans. Dielectr. Electr. Insul.*, vol. 23, no. 3, pp. 1506–1514, Jun. 2016.

[23] H. Yamasaki and S. Morita, "Identification of the epoxy curing mechanism under isothermal conditions by thermal analysis and infrared spectroscopy," *J. Mol. Struct.*, vol. 1069, pp. 164–170, Jul. 2014.

[24] S. Yoshida, "Quantitative evaluation of an epoxy resin dispersion by infrared spectroscopy," *Polym. J.*, vol. 46, no. 7, pp. 430–434, Jul. 2014.

[25] L. Dan and W. Yi-Hui, "Rapid identification of epoxy resin and phenolic resin using near infrared spectroscopy," *J. Near Infr. Spectrosc.*, vol. 25, no. 5, pp. 324–329, Oct. 2017.

[26] Y. Wang, S. Wang, Y. Huang, Y. Lu, and Y. Cai, "Study on thermal aging characteristics of epoxy resin of dry-type transformer," *High Voltage Eng.*, vol. 44, no. 1, pp. 187–194, 2018.

[27] G. Paul and W. Paul, "Identification of cellulosic fibres by FTIR spectroscopy: Differentiation of flax and hemp by polarized ATR FTIR," *Stud. Conservation*, vol. 51, no. 3, pp. 205–211, Jan. 2006.

YONGQIANG WANG was born in Hebei, China, in 1975. He received the B.Sc., M.S., and Ph.D. degrees in electrical engineering from North China Electric Power University, Baoding, China, in 1996, 2002, and 2009, respectively. He is engaged with teaching and his research interests are monitoring and fault diagnosis of electrical equipment, and electrical insulation technology.

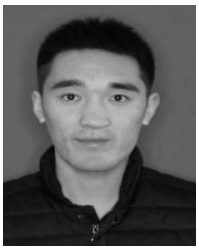

CHANGHUI FENG was born in Shandong, China, in 1995. He is currently pursuing the M.Sc. degree with North China Electric Power University, Baoding, China. His main research interest is monitoring and fault diagnosis of electrical equipment.

YU LUO was born in Hubei, China, in 1994. He is currently pursuing the M.Sc. degree with North China Electric Power University, Baoding, China. His main research interest is monitoring and fault diagnosis of electrical equipment.